RSC Advances

ROYAL SOCIETY OF CHEMISTRY

www.rsc.org/advances

Manuscript ID: RA-ART-12-2015-026913 R2

Effect of humic acid on the sulfamethazine adsorption by functionalized multi-walled carbon nanotubes in aqueous solution: mechanisms study

Quanquan Yang [a], Xiaogang Li [a], Guangcai Chen [a*], Jianfeng Zhang [a], Baoshan Xing [b]

[a] Research Institute of Subtropical Forestry, Chinese Academy of Forestry, Fuyang, Zhejiang 311400, China

[b] Stockbridge School of Agriculture, University of Massachusetts, Amherst, MA 01003, United States

* Corresponding author.

Phone: 86-571-63105079

Fax: 86-571-63141304

E-mail address: guangcaichen@sohu.com (Chen GC).

Abstract

Adsorption of humic acid (HA) and its effect on sulfamethazine (SMZ) adsorption by three types of multi-walled carbon nanotubes (MWCNTs) were investigated. The adsorption isotherms of HA and SMZ were well depicted by the Langmuir model (R^2>0.99). HA adsorption onto MWCNTs increased as pH decreased and ionic strength increased, and decreased with increasing surface oxygen content of MWCNTs, implying that electrostatic and hydrophobic interactions were the main adsorption mechanisms. The presence of HA inhibited SMZ adsorption onto MWCNTs via competitive interactions, molecular sieving, and pore blockage. HA adsorbed on the MWCNTs surfaces also altered the electrostatic and hydrophobic interactions between SMZ and MWCNTs, decreasing the adsorption of SMZ. The results of micro-Fourier transform infrared spectroscopy suggested that π-π and hydrogen-bonding interactions of MWCNTs with SMZ and HA, and/or between SMZ and HA also play an important role in the adsorption process. The current findings shed light on evaluating the potential utilization of MWCNTs in antibiotics removal or analysis.

.

Keywords: humic acid, sulfamethazine, adsorption, MWCNTs

1. Introduction

Antibiotics, an emerging group of environmental contaminant, are widely applied to prevent and treat disease in humans and farm animals. However, most of them are not totally absorbed and metabolized by humans or animals, and 50–90% are inevitably discharged into the environment via feces and urine [1, 2]. Sulfamethazine (SMZ), one of the major sulfonamide antibiotics, is widely used for treating infectious diseases and promoting the growth of farm animals. It is reported that SMZ concentrations in feedlot manure are up to 9990 μg kg^{-1} on a dry matter basis [2]. SMZ and other sulfonamides reach up to 900 mg kg^{-1} in manure [3]. SMZ residues are also widely detected in surface water [4], groundwater [5], and drinking water [6], with concentrations ranging from ng L^{-1} to μg L^{-1}. It has been suggested that SMZ may be carcinogenic, as thyroid tumors developed in rats and mice fed with 2.4–4.8 ppm SMZ over 24 months [7]. Therefore, continued research into the fate, distribution, biodegradation, and removal of SMZ is both important and necessary.

Many technologies, such as chemical oxidation/reduction, adsorption, and biological treatment, have been used for the removal of toxic pollutants, and the adsorption is considered to be one of most effective methods because convenience, highly efficient, and ease of operation [8]. Carbon nanotubes (CNTs) with a large specific surface area and pore volume [8, 9] which can serve as excellent adsorbent, enable CNTs the potential application in contaminants removal or analysis [10, 11].

Previous researches have investigated the adsorption of antibiotics onto CNTs and revealed various adsorption mechanisms. For example, hydrophobic interactions and

non-electrostatic π-π dispersion interactions are the main adsorption mechanisms responsible for the adsorption of tetracycline by CNTs [12]. However, electrostatic interactions play a key role in the adsorption of ciprofloxacin and norfloxacin onto CNTs [19, 20]. The adsorption of ciprofloxacin onto four types of CNTs increased as the pH increased from 0 to 7, then decreased as the pH increased from 7 to 14 [13]. Norfloxacin adsorption onto CNTs showed a similar trend with increasing pH [14], which was ascribed to changes in the electrostatic interactions between CNTs and contaminants due to the increase in pH. In general, antibiotics have multiple pK_a values and can exist as positive, zwitterionic, and negative species depending on solution pH. The contribution of different species to adsorption follows the order zwitterionic>positive>negative [15]. Zhang et al. calculated that neutral sulfamethoxazole contributes>80% to the overall adsorption [16]. Furthermore, adsorption of sulfamethoxazole onto CNTs is controlled by various mechanisms, including hydrophobic interactions, electrostatic interactions, hydrogen bonds, and π-π interactions [16-18]. Previous studies have shown that coexisting cations and anions also affect the adsorption of antibiotics by CNTs [17, 19].

Despite the great potential application, the toxicity of CNTs to organisms and their risks to environment raised lots of attention [20-22], which must be considered before using CNTs in contaminant adsorption or removal. Several pretreatment methods for CNTs are believed to be effective in alleviating or even avoiding the toxicity of CNTs. Purification of CNTs can reduce the cytotoxicity through releasing the metallic impurities containing in CNTs which are toxic to cell [23]. Surface functionalization

with carboxylic acid (-COOH) or ammonium can reduce the toxicity although increasing the biocompatibility and dispersibility of CNTs [24]. It was observed that functionalized CNTs even shown no toxicity in vitro to cells and in vivo in mice [25]. Natural organic matter (NOM) is suggested to reduce the toxicity of CNTs to bacteria through coating [26], or show no toxicity to *Daphnia magna* through stabilizing the CNTs in solution [27]. Thus, understanding the interaction between NOM and CNTs is essential for reducing or avoiding toxicity of CNTs while using them for toxicants removal. In addition, the presence of NOM can also affect the adsorption of contaminant by CNTs.

However, research on the effect of natural organic matter (NOM) on the adsorption of antibiotics onto CNTs is limited. NOM is ubiquitous in the environment, and antibiotic is an emerging group of environmental contaminant; they can coexist in both water and soil environments. Understanding the effect of NOM on the adsorption of antibiotics by CNTs is crucial for assessing the fate of antibiotics in the environment. In general, competitive interactions and pore blockage are considered to be the two major mechanisms by which NOM inhibits the adsorption of organic contaminants by CNTs [28, 29]. Although the presence of NOM could increase the total adsorption sites on CNT surfaces owing to better dispersion of CNTs, adsorption reduces significantly because of a decrease in the number of available sites for contaminants due to competition and blockage [30]. Furthermore, humic acid (HA) adsorbed onto CNT surfaces introduces polar moieties and lowers the point of zero charge, which decreases adsorption via hydrophobicity and electrostatic interactions [29,

[31]. Therefore, it is important to examine the effect of NOM on the interface interactions between antibiotics and CNTs in solution.

In this study, we selected HA and SMZ as the model NOM and antibiotic, respectively. Three multi-walled carbon nanotubes (MWCNTs) with different surface oxygen contents were chosen as the adsorbents. The objectives of this study were to: (i) examine the effect of solution pH and ionic strength on the adsorption of HA by MWCNTs; (ii) elucidate the effect of HA on the adsorption of SMZ by MWCNTs; and (iii) provide spectroscopic evidence of the adsorption mechanisms using micro-Fourier transform infrared (μ-FTIR) spectroscopy.

2. Materials and methods

2.1. Materials

The three adsorbents were pristine, carboxylated, and hydroxylated MWCNTs (P-MWCNT, C-MWCNT, and H-MWCNT) with outer diameters of 10–20 nm. The MWCNTs were synthesized by chemical vapor deposition of methane in hydrogen at 700°C using Ni as the catalyst (Chengdu Organic Chemistry Co. Ltd, Chinese Academy of Sciences). The surface carbon and oxygen elemental composition of the MWCNTs was determined by X-ray photoelectron spectroscopy (Thermo ESCALAB 250Xi, UK). The zeta potential versus solution pH was recorded using a zeta potential analyzer (Nano-Z, Malvern Instruments, UK). The μ-FTIR spectroscopic spectra of the three MWCNTs were measured using a FTIR spectrophotometer (Nicolet 6700, Thermo Nicolet).

SMZ (purity>99%) and HA were purchased from Sigma-Aldrich Trading Co. Ltd

(Shanghai, China). The molecular structure and physicochemical properties of SMZ are listed in Table S1. Elemental composition and relative carbon contributions of HA are presented in Table S2. All other chemicals and solvents were of analytical reagent grade or better.

2.2. Adsorption experiments

All experiments were carried out in 40 mL glass vials sealed with Teflon-lined screw caps. The vials were filled with 5 mg of MWCNTs and 25 mL of background solution containing 0.02 M $NaNO_3$ and 200 mg L^{-1} NaN_3. The reaction solutions with various SMZ and HA concentrations were suspended in a shaker (HZQ-F160, Huamei Biochemistry Instrument, Soochow) with a rotation speed of 150 rpm at 298K in the dark. According to preliminary adsorption kinetics experiments, the adsorption reached equilibrium within 72h (Figure S1).The suspension solutions were filtered using a 0.45 μm hydrophilic membrane and the SMZ and HA concentrations in the supernatants were determined. Each treatment was carried out in triplicate.

2.2.1 Adsorption isotherms

A 200 mg L^{-1} HA stock solution was prepared by dissolving 200 mg HA in 10 mL 0.1 M NaOH and diluting to 1L. The pH was adjusted to pH 7 using 0.1M HNO_3. The HA stock solution was diluted further to obtain a series of initial concentrations varying from 5 to 100 mg L^{-1} for adsorption experiments.

2.2.2 Effect of pH on adsorption

The effect of solution pH on HA adsorption at a HA concentration of 40 mg L^{-1} was investigated by varying the pH from 3 to 11. During the reaction, solutions were

readjusted by 0.1M NaOH or HNO_3 at 2, 12, and 22 h to ensure that the difference between initial and final pH was<0.1.

2.2.3 Effect of ionic strength on adsorption

To investigate the effect of ionic strength on HA adsorption, 0.01M and 0.1M $NaNO_3$were used at HA concentrations varying from 10 to 80 mg L^{-1}at a solution pH of 7. The effect of ionic strength on adsorption of SMZ by MWCNTs has been investigated in a previous study [19].

2.2.4 Effect of HA on SMZ adsorption

Simultaneous adsorption experiments were conducted at initial SMZ concentrations varying from 2 to 100 mg L^{-1} with HA concentrations of 0, 10, and 30 mg L^{-1}. All the adsorption isotherm experiments were carried out at pH 7.

2.2.5 Solubility of SMZ

The solubility of SMZ was determined by adding an excess of SMZ to the background solution, and at 10 and 30 mg L^{-1} HA (pH 2 to 11). Briefly, 100 mg SMZ was weighed in a 25 ml brown bottle containing 20 mL background solution. Subsequently, the solution pH was adjusted accordingly using 0.1M NaOH or HNO_3. The solution was sonicated in a water bath for 10 min and rotated in a shaker at 150 rpm for 72 h at 298 K in the dark. Then the same samples were filtered using 0.22 μm and 0.45 μm membrane after centrifugation at 1000*g* for 60 min, and the supernatant was used for SMZ concentration determination using high-performance liquid chromatography (HPLC, Waters Alliance). Figure S2 shown that the solubility of SMZ filtered by 0.22 μm only is a little larger than by 0.45 μm, the fluctuation range

177 <0.03. The influence of SMZ particle passed through membrane on SMZ solubility
178 can be ignored.

179 2.3. Analysis

180 Supernatants were centrifuged for 10 min at 1000 *g* and then filtered through a
181 0.45 μm hydrophilic membrane before HA or SMZ concentration determination. HA
182 has both hydrophilic and hydrophobic moieties owing to its complex structure and
183 wide range of molecular weight [32]. HA with different structures usually selectively
184 adsorb onto CNTs [33], which may make the single-wavelength method inaccurate for
185 the determination of HA concentration in equilibrium solution. To eliminate this
186 possible inaccuracy, the HA absorbance spectrum in the initial (equilibrium) solution
187 was obtained using a 1800 PC ultraviolet-visible (UV)spectrophotometer (Shanghai
188 Mapada Instrument Co. Ltd). The results showed no difference in the HA adsorption
189 peak before and after adsorption (Figure S3). HA concentrations in the range 4 to 40
190 mg L^{-1} linearly correlated with UV absorbance (R^2 >0.99; Figure S4) at 254 nm in a 1
191 cm quartz cell [34]. This indicated that using a spectrophotometer at 254 nm was reliable
192 for determining HA concentration.

193 The SMZ concentration in the supernatants was determined using HPLC equipped
194 with a Waters 484 UV detector at 263 nm and a reverse-phase C18 column (Waters,
195 5 μm, 3.9 mm×150 mm). The mobile phase was methanol and water with a volume
196 ratio of 70:30. The injection volume was 30 μL and the flow rate was 1 $mLmin^{-1}$. The
197 retention time was 1.5 min.

198 2.4. Data analysis

The equilibrium adsorption data for HA and SMZ fitted the Langmuir (Eq. 1) and Freundlich (Eq. 2) models:

$$q_e = \frac{q_m b c_e}{1 + b c_e} \quad (1)$$

$$q_e = k_F c_e^{1/n} \quad (2)$$

where q_e(mg g^{-1}) is the adsorption amount at equilibrium, q_m (mg g^{-1}) is the maximum adsorption capacity, c_e (mg L^{-1}) is the equilibrium concentration in solution, b (L mg^{-1}) is the affinity parameter, k_F ($mg^{(1-(1/n))}g^{-1}L^{(1/n)}$) is the adsorption coefficient, and n is the adsorption constant as an indicator of isotherm nonlinearity.

3. Results and discussion

3.1. Characterization of MWCNTs

The specific surface areas of P-MWCNT, C-MWCNT, and H-MWCNT were similar due to the same outer diameter (Table S3, [35]). The C1s (~294–282 eV) and O1s (~537–528 eV) peaks of the MWCNTs deconvoluted from X-ray photoelectron spectroscopy data revealed the functional groups (Figure 1).The three MWCNTs showed the same main peaks at 284.4 and 285.5 eV assigned to sp^2 C=C (attributed to the graphitic structure) and sp^3 C–C (attributed to defects in the nanotube structure), respectively [36]. Small peaks for O–COO (290.9 eV) and C=O (288.2 eV) were attributed to carbon atoms attached to different oxygen-containing moieties [37]. For O1s, the peaks at 533.6 eV were C–O–C, C–O–OH, and C–OH; the peaks at 532.5 eV were C=O and O–C=O; the peaks at 531.3 eV were isolated –OH, C=O, and O–C=O; the peaks at 530.7 eV were physically adsorbed O or carbonates [36].

The μ-FTIR spectra also confirmed the different oxygen functional groups (Figure S5). The peaks at 1192 cm^{-1} and 1027 cm^{-1} (P-MWCNT), 1200 cm^{-1} and 1064 cm^{-1}

(C-MWCNT), and 1207 cm^{-1} and 1062 cm^{-1} (H-MWCNT) were assigned to the C–O stretching vibration [35, 38, 39]. The peaks at 1706 cm^{-1} (C-MWCNT) and 1705 cm^{-1} (H-MWCNT) were assigned to the C=O stretching vibration of COOH. The peaks in the region ~3820–3420 cm^{-1} corresponded to OH groups (Figure S5). These oxygen-containing functional groups are hydrophilic, and thus decrease the hydrophobicity of the MWCNT surface.

The zeta potential of the MWCNTs decreased with increasing solution pH from 1 to 13 (Figure S6). The point of zero charge of P-MWCNT, C-MWCNT, and H-MWCNT was 1.7, 2.5, and 4.5, respectively. The zeta potential also reduced with increasing surface oxygen content at the same solution pH, which was ascribed to deprotonation of carboxylic groups, making the MWCNT surface more negatively charged [35].

3.2 Adsorption of HA onto MWCNT

The HA adsorption isotherms of the three different MWCNTs fitted the Langmuir and Freundlich models (Figure 2a, Table 1). The Langmuir model fitted the adsorption data better than the Freundlich model with a higher R^2 value (Table 1). The maximum HA adsorption capacities of the three MWCNTs followed the order: P-MWCNT>C-MWCNT>H-MWCNT (Table 1), which suggests that an increase in surface oxygen content decreases the adsorption of HA onto MWCNTs (Table S2). Previous studies have shown that π-π, hydrophobic, and electrostatic interactions are the predominant mechanisms for the adsorption of organic matter [34, 40]. As the number of hydrophilic oxygen-containing functional groups increases, the aromatic content of

MWCNTs decreased, which could weaken the π-π interactions between HA and MWCNTs [41]. These functional groups create a polar region, and reduce the hydrophobicity of the MWCNT surface [20], which could decrease the HA adsorption by MWCNTs. In addition, HA contains many functional groups that are easily negatively charged, and MWCNTs with high oxygen content are more negatively charged, making adsorption more difficult due to electrostatic repulsion between HA and the negatively charged MWCNT surface [41].

The HA adsorption steeply decreased as solution pH increased (Figure 2b). Generally, solution pH is an important factor affecting the adsorption of HA by CNTs, which can affect the interaction between functional groups of CNTs and HA, and the humic acids molecules structure [42, 43]. HA has negative charges under the solution pH of experimental conditions [10, 44]. The surface of the MWCNTs positively charged at low solution pH, but negatively charged at high solution pH (Figure S6). Thus, the adsorption of HA onto the MWCNTs occurred easily at low pH through electrostatic attractions, and then became difficult due to the electrostatic repulsion between the negative charges of MWCNTs and HA at high pH [45]. In addition, at high solution pH, the deprotonation of acidic functional groups in HA, such as carboxyl and phenolic groups, could increase the hydrophilicity, which may suppress adsorption of HA by MWCNTs through hydrophobic interactions [46]. Hydrogen-bonding interactions between HA and MWCNTs, which was confirmed by the μ-FTIR spectra (Section 3.4), decreased with increasing solution pH. As pH increases, HA molecules become less coiled and less compact because of electrostatic repulsions [47], resulting in HA

occupying more sites on MWCNT surface. Therefore, the effect of solution pH on the adsorption process was the result of a combination of aforementioned mechanisms.

As the ionic strength increased from 0.01 to 0.1M, the HA adsorption increased by 15–20%, 22–53%, and 43–96% for P-MWCNT, C-MWCNT, and H-MWCNT, respectively (Figure 3). This implies that electrostatic interactions were the main adsorption mechanism. An increase in ionic strength can screen the surface charge of MWCNTs [48], thus reducing the electrostatic repulsion between the MWCNTs and HA and increasing the adsorption of HA onto the MWCNTs. The increase was strongly and positively correlated with the oxygen content of the MWCNTs due to the larger charge screening effects on these MWCNTs with higher oxygen content. The ionic strength can also alter macromolecular configurations of HA, which in turn affects the adsorption of HA onto MWCNTs. The molecular configurations of HA became more coiled and compact with increasing ionic strength [44, 49], leading to more HA molecules occupying the same surface sites of MWCNTs [50]. At higher ionic strengths, the double layer compression of MWCNT–HA agglomerates can be enhanced, and the adsorption capacity also increases [33].

The results suggested that MWCNTs surface oxygen contents and solution properties (pH and ionic strength) can affect the adsorption process of both HA and SMZ onto MWCNTs. The main mechanisms were ascribed to the hydrophobic and electrostatic interactions which dominated the adsorption behavior. The hydrophobic interaction decreased with the increase of surface oxygen contents due to the introduction of O-containing functional group in MWCNTs surface. The electrostatic

interactions between MWCNTs and HA/SMZ were affected by the ionization level of functional groups of MWCNTs, HA, and SMZ, which was dependent on solution pH. Salt ions can also affect the electrostatic interaction between MWCNTs and HA/SMZ through the charge shielding effect.

3.3 Effect of HA on the adsorption of SMZ onto MWCNTs

The effect of HA on the adsorption of SMZ onto MWCNTs was investigated (Figure 4, Table 2). The adsorption of SMZ was nonlinear and fitted the Langmuir model well (R^2 >0.99). The presence of HA suppressed the adsorption of SMZ onto the MWCNTs, and the degree of inhibition increased with increasing HA concentration (Figure 4). The SMZ adsorption onto the three MWCNTs decreased by 8.3–11.9% at 10 mg L^{-1} HA, and 13.8–19.4% at 30 mg L^{-1} HA. This result can be explained by the direct competition for adsorption sites between HA and SMZ [28], which made the adsorption of SMZ onto the MWCNT surface more difficult. Figure S7a shown that 68.3-61.5 % HA was precipitated by 5 mM Ca^{2+}, and recovery percentage of SMZ (Figure S7b) suggests that the adsorption of SMZ onto HA was small and can be ignored in this study, indicating that SMZ is directly adsorbed onto the surface of MWCNTs [51]. In addition, HA adsorbed onto MWCNTs increases the negative charge density on the surface of MWCNTs [25], increasing the electrostatic repulsion between SMZ and HA-coated MWCNTs, thus decreasing SMZ adsorption. Molecular sieving and pore blockage caused by HA can also suppress SMZ adsorption [52]. HA can improve the dispersion of MWCNTs, leading to the formation of a stable MWCNT suspension in aqueous solution [46, 53]. However, the suspension of

MWCNTs is largely based on continuing sonication. In this study, HA may not have increased the number of available adsorption sites on the MWCNT surfaces for SMZ due to the lack of sonication [28]. On the other hand, the increase in the number of available adsorption sites could have been offset by the adsorption of HA. In sum, the addition of HA reduced the adsorption of SMZ onto the MWCNTs in this study.

Solubilization effects may reduce SMZ adsorption onto CNTs by increasing the mobility and desorption of chemicals from CNTs, and always act simultaneously with competition effects [53]. To explore the contribution of solubilization in the present study, the solubility of SMZ at pH 2 to 11 was also examined. Figure 5 shows that the solubility of SMZ decreased with increasing solution pH, reaching a minimum value at pH 6, and then increased with increasing solution pH. The fluctuation range of SMZ solubility in the presence of 10 and 30 mg L^{-1} HA was < 0.05 compared with that in background solution, which implied that solubilization effects were insignificant (Figure S8).

The effect of HA concentration on the adsorption of SMZ onto MWCNTs at different pHs was investigated (Figure 6). In the presence of HA, SMZ adsorption was inhibited at low solution pH, while adsorption was enhanced at pH>9. The suppression effect increased with increasing HA concentration in solution. SMZ, an ionizable compound, has two pK_a values of 2.28 and 7.42 (Table S2). The speciation of SMZ depended on solution pH (Figure S9) [55, 56]. Previous studies have found that electrostatic interactions also depend strongly on solution pH [40], while π-π interactions are independent of solution pH [57]. Our previous study suggested that

SMZ adsorption onto MWCNTs is governed by electrostatic and π-π interactions [19].

At low solution pH, the adsorption of SMZ onto MWCNTs was high; however, the electrostatic repulsions and competitive interactions increased with the addition of HA, suppressing SMZ adsorption onto the MWCNTs. At solution pH>9, HA has high solubility and high mobility, which weaken the competition effect. And at this pH region, the SMZ adsorption was inherently lower. SMZ is negatively charged, and adsorption is accompanied by proton exchange, a major driving force is strong negative charge-assisted H-bonding [(-)CAHB interaction between SMZ and acidic surface groups of MWCNTs [58, 59]. Humic acid molecules containing acid functional groups [29], which may enhance the H-bonding interaction, promote the adsorption of SMZ onto the MWCNTs. Considering the significantly different effects of HA on the SMZ adsorption by MWCNTs at different solution pH, more attention should be paid to solution chemistry during SMZ removal or analysis by MWCNTs.

3.4 μ-FTIR analysis

The μ-FTIR spectra of the MWCNTs, MWCNT–SMZ, MWCNT–HA, and MWCNT–SMZ–HA were recorded to reveal the mechanisms of SMZ and HA adsorption onto the MWCNTs (Figure 7). Some additional peaks appeared at ~1640–1580cm^{-1} in the MWCNT–SMZ spectrum (Figure 7b) compared with the free MWCNTs (Figure 7a). The peaks at 1636 cm^{-1}, 1630 cm^{-1}, and 1635 cm^{-1} were assigned to the C=N stretching vibration of SMZ [60], indicating that the SMZ was adsorbed onto the MWCNT surface. After SMZ was adsorbed onto the MWCNTs, the peaks corresponding to the C=C stretching vibration and the C–C skeletal vibration of

the benzene ring shifted from 1514 cm^{-1} and 1392 cm^{-1} to 1509 cm^{-1} and 1390 cm^{-1} for P-MWCNT, from 1506 cm^{-1} and 1387 cm^{-1} to 1510 cm^{-1} and 1389 cm^{-1} for C-MWCNT, and from 1552 cm^{-1} and 1382 cm^{-1} to 1527 cm^{-1} and 1394 cm^{-1} for H-MWCNT, respectively [61]. The MWCNT–HA spectrum (Figure 7c) showed that the C=C and C–C vibrations of the benzene ring have a similar shift after the adsorption of HA: the C=C stretching vibration shifted from 1514 cm^{-1} to 1553 $cm^{-1}$for P-MWCNT, from 1506 cm^{-1} to 1557 cm^{-1} for C-MWCNT, and from 1552 cm^{-1} to 1562 cm^{-1} for H-MWCNT; and the C–C skeletal vibration shifted from 1392 cm^{-1} to 1365 cm^{-1}, from 1387 cm^{-1} to 1384 cm^{-1}, and from 1382 cm^{-1} to 1380 cm^{-1} for P-MWCNT, C-MWCNT, and H-MWCNT, respectively. All of these shifts suggest that π-π interactions play an important role in the adsorption of SMZ and HA onto MWCNTs [62]. The MWCNT–SMZ–HA spectrum (Figure 7d) showed that the co-adsorption of SMZ and HA onto the MWCNTs induced more significant changes in the μ-FTIR spectrum of MWCNTs.

For P-MWCNT, the C–O stretching vibration peak at 1192 cm^{-1} was shifted to 1199 cm^{-1} (MWCNT–SMZ), 1202 cm^{-1} (MWCNT–HA), and 1203 cm^{-1} (MWCNT–SMZ–HA), which can be attributed to the interactions between C–O and the benzene ring. For C-MWCNT, the C=O stretching vibrations peak at 1706 cm^{-1} and the C–O stretching vibration peak at 1200 cm^{-1} were shifted to 1711 cm^{-1} and 1198 cm^{-1} (MWCNT–SMZ), 1716 cm^{-1} and 1203 cm^{-1} (MWCNT–HA), and 1708 cm^{-1} and 1197 cm^{-1} (MWCNT–SMZ–HA), respectively. For H-MWCNT, the stretching vibrations of C=O and C–O were shifted from 1705cm^{-1} and 1207cm^{-1} to

1717 cm^{-1} and 1201 cm^{-1} (MWCNT–SMZ), 1715 cm^{-1} and 1205 cm^{-1} (MWCNT–HA), and 1699 cm^{-1} and 1212 cm^{-1} (MWCNT–SMZ–HA), respectively. All of these band shifts verify that SMZ, HA, and SMZ and HA were partly adsorbed onto the MWCNTs by hydrogen bonding via the C=O or -COO- groups [39].

4. Conclusion

The adsorption of SMZ and HA onto MWCNTs decreased as the surface oxygen content increased, due to weakening of the π-π and hydrophobic interactions of MWCNTs with SMZ or HA. The HA adsorption onto MWCNTs also depended on solution pH and ionic strength, suggesting that electrostatic interactions play a key role in the adsorption of HA onto MWCNTs. This work confirmed that the presence of HA suppresses SMZ adsorption onto MWCNTs at a wide pH range, which can be ascribed to competitive interactions, molecular sieving, and pore blockage. The μ-FTIR spectra validated that π-π and hydrogen-bonding interactions are the main mechanisms for the adsorption of SMZ and HA onto MWCNTs. The current findings shed light on evaluating the potential utilization of MWCNTs in antibiotics removal or analysis.

Acknowledgment

This work was funded by the National natural Science Foundation of China (21207157), and USDA-AFRI Hatch program (MAS 00475).

Appendix A. Supplementary data

Supplementary data related to this article are provided.

References

1 S.T. Kurwadkar, C.D. Adams, M.T. Meyer, D.W. Kolpin, *J. Agr. Food Chem.*, 2007, 55, 1370.

2 M.O. Aust, F. Godlinski, G.R. Travis, X. Hao, T.A. McAllister, P. Leinweber, S. Thiele-Bruhn, *Environ. Pollut.*, 2008, 156, 1243.

3 M. Teixido, C. Hurtado, J.J. Pignatello, J.L. Beltran, M. Granados, J. Peccia, *Environ. Sci. Technol.*, 2013, 47, 6197.

4 F. Tamtam, F. Mercier, B. Le Bot, J. Eurin, Q. Tuc Dinh, M. Clément, M. Chevreuil, *Sci. Total. Environ.*, 2008, 393, 84.

5 G. Hamscher, H.T. Pawelzick, H. Höper, H. Nau, *Environ. Toxicol. Chem.*, 2005, 24, 861.

6 A.J. Watkinson, E.J. Murby, D.W. Kolpin, S.D. Costanzo, *Sci. Total. Environ.*, 2009, 407, 2711.

7 W. Lertpaitoonpan, S.K. Ong, T.B. Moorman, *Chemosphere*, 2009, 76, 558.

8 J.G. Yu, X.H. Zhao, H. Yang, X.H. Chen, Q. Yang, L.Y. Yu, J.H. Jiang, X.Q. *Chen, Sci. Total. Environ.,* 2014, 482-483, 241.

9 K. Yang, B. Xing, *Environ. Pollut.,* 2007, 145, 529.

10 X. Tian, T. Li, K. Yang, Y. Xu, H. Lu, D. Lin, *Chemosphere,* 2012, 89, 1316.

11 A. Deb, B. Mohanty, P. Ilaiyaraja, K. Sivasubramanian, B. Venkatraman, *J. Radioanal. Nucl. Chem.*, 2012, 295, 1161.

12 L. Zhang, X. Song, X. Liu, L. Yang, F. Pan, J. Lv, *Chem. Eng. J.*, 2011, 178, 26.

13 H. Li, D. Zhang, X. Han, B. Xing, *Chemosphere*, 2014, 95, 150.

14 Z. Wang, X. Yu, B. Pan, B. Xing, *Environ. Sci. Technol.*, 2009, 44, 978.

15 X. Yu, L. Zhang, M. Liang, W. Sun, *Chem. Eng. J.*, 2015, 279, 363.

16 Z. Di, P. Bo, Z. Huang, N. Ping, X. Baoshan, *Environ. Sci. Technol.*, 2010, 44, 3806.

17 D. Zhang, B. Pan, M. Wu, B. Wang, H. Zhang, H. Peng, D. Wu, P. Ning, *Environ. Pollut.*, 2011, 159, 2616.

18 D. Wu, B. Pan, M. Wu, H. Peng, D. Zhang, B. Xing, *Sci. Total Environ.*, 2012, 427-428, 247.

19 Q. Yang, G. Chen, J. Zhang, H. Li., *RSC Adv.*, 2015, 5, 25541.

20 W.L. Sun, J. Xia, S. Li, F. Sun, *Chem. Eng. J.*, 2012, 200-202, 627.

21 E. Navarro, A. Baun, R. Behra, N.B. Hartmann, J. Filser, A.J. Miao, A. Quigg, P.H. Santschi, L. Sigg, *Ecotoxicology*, 2008, 17, 372.

22 Q. Mu, G. Jiang, L. Chen, H. Zhou, D. Fourches, A. Tropsha, B. Yan, , *Chem. Rev*, 2014, 114, 7740.

23 R. J. Toh, A. Ambrosi, M. Pumera, Chemistry, 2012, 18, 115936.

24 S.Y. Madani, A. Mandel, A.M. Seifalian, Nano. Rev., 2013, 4, 21521.

25 Z. Liu, S. Tabakman, K. Welsher, H. Dai, Nano Res., 2009, 2, 85120.

26 R. Su，Y. Jin，Y. Liu，M. Tong，H. Kim, Colloids & Surfaces B Biointerfaces, 2013, 104(4):133-139].

27 K.T. Kim, A. J. Edgington, S. J. Klaine, J.W. Cho, S. D. Kim, Environ. Sci. Technol. 2009, 43, 8979].

28 F. Wang, J. Yao, C. Yu, H. Chen, Z. Yi, M.M.F. Choi, *ACS Sustain. Chem. Eng.,* 2014, 2, 1219.

29 T. Huffer, S. Schroth, T.C. Schmidt, *Chemosphere*, 2015, 119, 1169.

30 S. Zhang, T. Shao, T. Karanfil, *Water Res.*, 2011, 45, 1378.

31 D. Lin, X. Tian, T. Li, Z. Zhang, X. He, B. Xing, *Environ. Pollut.*, 2012, 167, 138.

32 W. Wu, H. Sun, L. Wang, K. Li, L. Wang, *J. Hazard. Mater.*, 2010, 174, 635.

33 H. Hyung, J.-H. Kim, *Environ. Sci. Technol.*, 2008, 42, 4416.

34 X. Wang, L. Shu, Y. Wang, B. Xu, Y. Bai, S. Tao, B. Xing, *Environ. Sci. Technol.*, 2011, 45, 9276.

35 G.C. Chen, X.Q. Shan, Y. Zhou, X. Shen, H. Huang, S. Khan, *J. Hazard. Mater.*, 2009, 169, 912.

36 V. Datsyuk, M. Kalyva, K. Papagelis, J. Parthenios, D. Tasis, A. Siokou, I. Kallitsis, C. Galiotis, *Carbon*, 2008, 46, 833.

37 G.C. Chen, X.Q. Shan, Y.S. Wang, B. Wen, Z.G. Pei, Y.N. Xie, T. Liu, J.J. Pignatello, *Water Res.*, 2009, 43, 2409.

38 A. Deb, P. Ilaiyaraja, D. Ponraju, B. Venkatraman, *J. Radioanal. Nucl. Chem.*, 2012, 291, 877.

39 G.C. Chen, X.Q. Shan, Z.G. Pei, H. Wang, L.R. Zheng, J. Zhang, Y.N. Xie, *J. Hazard. Mater.*, 2011, 188, 156.

40 K. Yang, B. Xing, *Environ. Pollut.*, 2009, 157, 1095.

41 B. Smith, J. Yang, J.L. Bitter, W.P. Ball, D.H. Fairbrother, *Environ. Sci. Technol.*, 2012, 46, 12839.

42 S.P. Moussavi, M.H. Ehrampoush, A.H. Mahvi, M. Ahmadian, S. Rahimi, *Asian J. Chem.*, 2013, 25, 5319.

43 S.P. Moussavi, M.H. Ehrampoush, A.H. Mahvi, S. Rahimi, M. Ahmadian, *Asian J. Chem.*,

458 2014, 26, 821.
459 44 K. Ghosh, M. Schnitzer, *Soil Sci.*, 1980, 129, 266.
460 45 G. Sheng, J. Li, D. Shao, J. Hu, C. Chen, Y. Chen, X. Wang, *J. Hazard. Mater.*, 2010, 178, 333.
461 46 D. Lin, T. Li, K. Yang, F. Wu, *J. Hazard. Mater.*, 2012, 241-242, 404.
462 47 F. Wang, J. Yao, H. Chen, Z. Yi, B. Xing, *Environ. Pollut.*, 2013, 180, 1.
463 48 D. Lin, N. Liu, K. Yang, L. Zhu, Y. Xu, B. Xing, *Carbon*, 2009, 47, 2875.
464 49 C. Lu, F. Su, *Sep. Purif. Technol.*, 2007, 58, 113.
465 50 J.E. Kilduff, T. Karanfil, W.J. Weber, *Environ. Sci. Technol.*, 1996, 30, 1344.
466 51 F.F. Liu, J. Zhao, S. Wang, P. Du, B. Xing, *Environ. Sci. Technol.*, 2014, 48, 13197.
467 52 L. Hou, D. Zhu, X. Wang, L. Wang, C. Zhang, W. Chen, *Environ. Toxicol. Chem.*, 2013, 32,
468 493.
469 53 D. Zhang, B. Pan, R.L. Cook, B. Xing, *Environ. Pollut.*, 2015, 196, 292.
470 54 J. Zhao, Z. Wang, H. Mashayekhi, P. Mayer, B. Chefetz, B. Xing, *Environ. Sci. Technol.*, 2012,
471 46, 5369.
472 55 L. Zhang, T. Xu, X. Liu, Y. Zhang, H. Jin, *J. Hazard. Mater.*, 2011, 197, 389.
473 56 L. Zhang, X. Song, X. Liu, L. Yang, F. Pan, J. Lv, *Chem. Eng. J.*, 2011, 178, 26.
474 57 W. Chen, L. Duan, D. Zhu, *Environ. Sci. Technol.*, (2007) 41, 8295.
475 58 M. Teixidó, J.J. Pignatello, J.L. Beltrán, M. Granados, J. Peccia, *Environ. Sci. Technol.*, 2011,
476 45, 10020.
477 59 X. Li, B. Gamiz, Y. Wang, J.J. Pignatello, B. Xing, *Environ. Sci. Technol.*, 2015, 49, 1409.
478 60 A.M. Mansour, *J. Coord. Chem.*, 2013, 66, 1118.
479 61 V. Udayakumar, S. Periandy, S. Ramalingam, *Spectrochim.Acta Part A*, 2011, 79, 920.
480 62 J. Wang, Z. Chen, B. Chen, Environ. *Sci. Technol.*, 2014, 48, 4817.
481
482
483
484
485
486

Captions

Fig. 1. The C1s and O1s X-ray photoelectron spectroscopy spectra of P-MWCNT, C-MWCNT, and H-MWCNT.

Fig. 2. Adsorption of HA by P-MWCNT (□), C-MWCNT (○), and H-MWCNT (Δ). (a) Adsorption isotherms (temperature: 298 K; initial pH: 7.0 ± 0.1). The solid line is the Freundlich model isotherm and the dotted line is the Langmuir model isotherm. (b) Effect of pH on adsorption (initial HA concentrations 40 mg/L; temperature: 298 K).

Fig. 3. Effect of ionic strength (initial pH: 7.0 ± 0.1; temperature: 298 K). (a) Adsorption of HA by P-MWCNT (□ ■), C-MWCNT (○●), and H-MWCNT (Δ ▲) at ionic strengths of 0.01 (□ ○ Δ) and 0.1 M (■ ● ▲) $NaNO_3$. (b) Ratio of adsorption capacity of 0.1 M and 0.01 M $NaNO_3$.

Fig. 4. Adsorption isotherms of SMZ without and with HA for P-MWCNT (a), C-MWCNT (b), and H-MWCNT (c) (temperature: 298K; initial pH: 7.0 ± 0.1). The solid line is the Freundlich model isotherm and the dotted line is the Langmuir model isotherm.

Fig. 5. SMZ Solubility as a function of solution pH in the absence and presence of HA at 10 and 30 mg/L.

Fig. 6. Adsorption of SMZ onto P-MWCNT (a), C-MWCNT (b), and H-MWCNT (c) as a function of pH in the absence and presence of HA at 10 and 30 mg/L (initial concentration of SMZ 20 mg/L; temperature: 298 K).

Fig. 7. The μ-FTIR spectra of MWCNTs(a), SMZ adsorbed onto MWCNTs (b), HA adsorbed onto MWCNTs(c), and SMZ–HA complexes on MWCNTs (d).

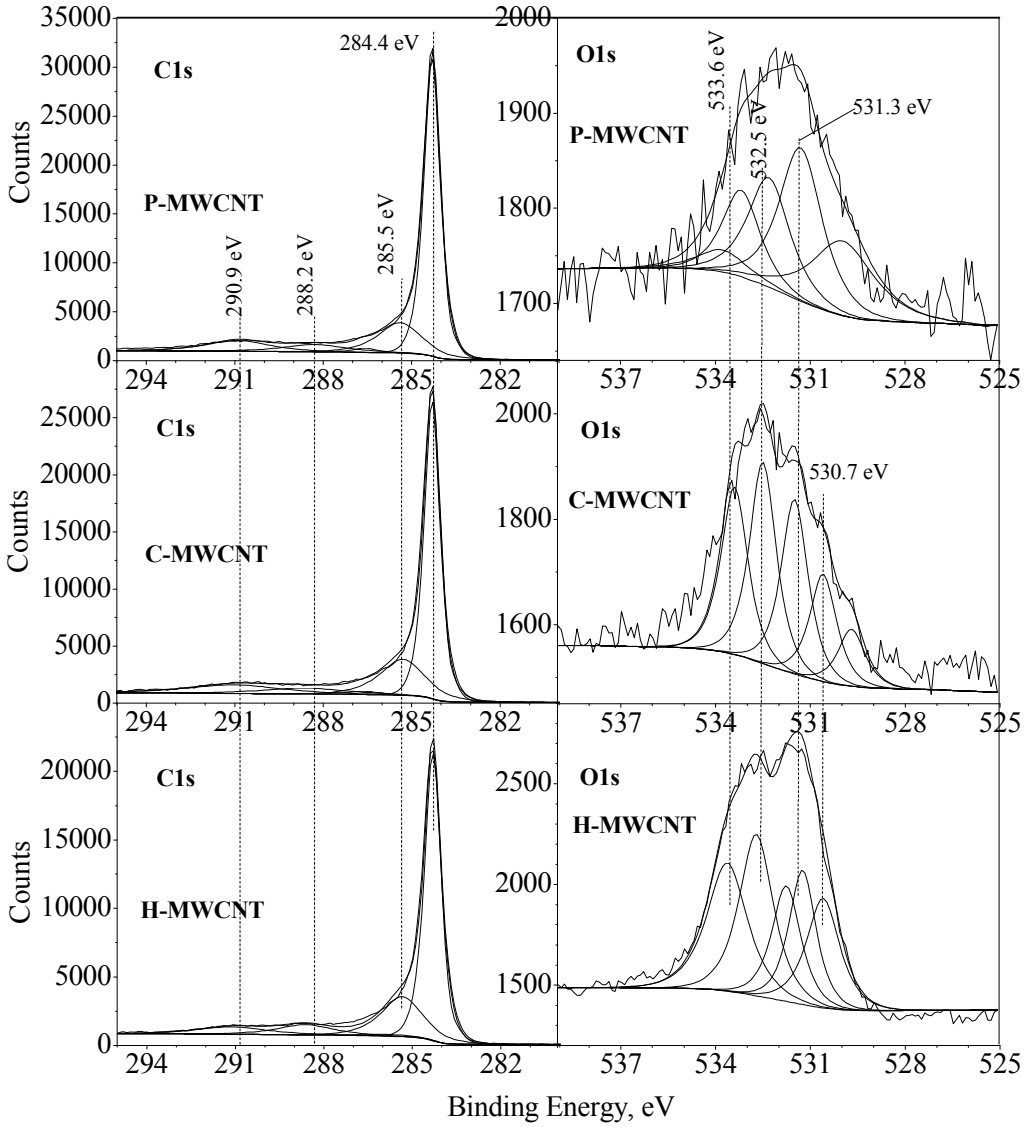

509

510 **Fig. 1.**

511

512

513

514

515

516

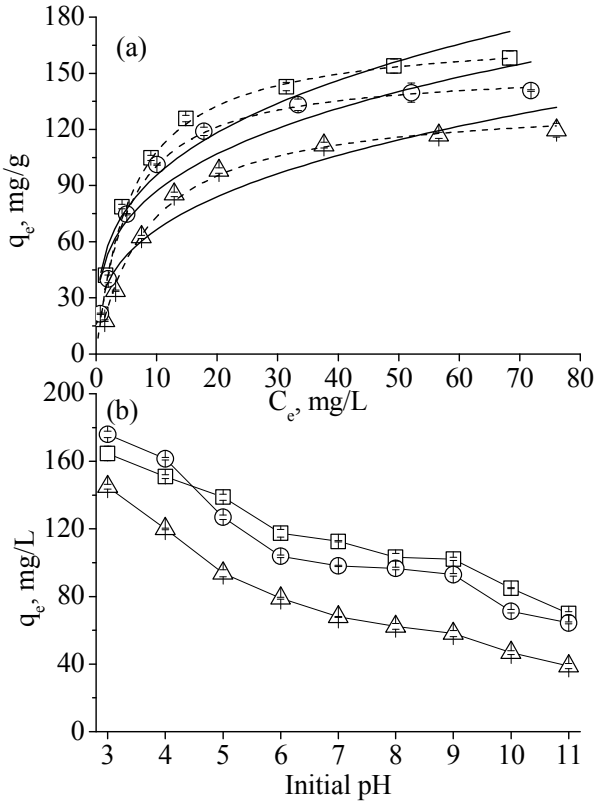

517

518 **Fig. 2.**

519

520

521

522

523

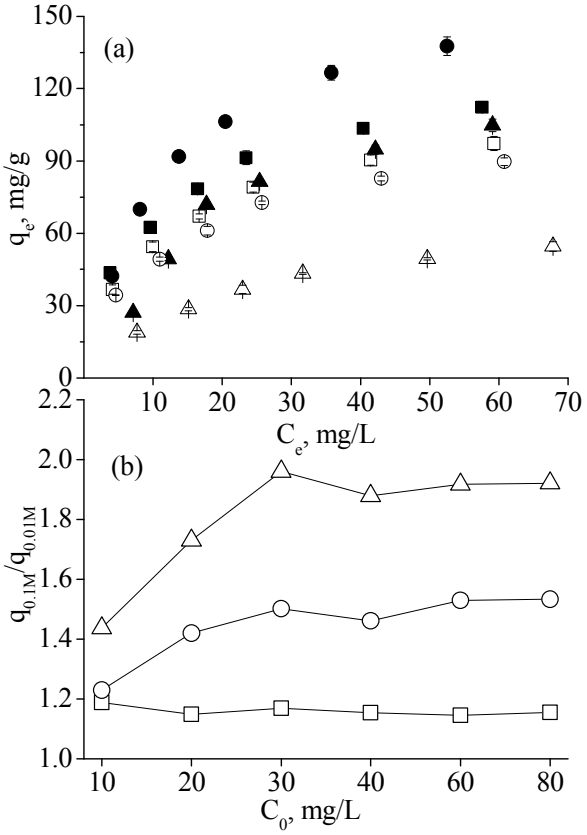

524

525 **Fig. 3.**

526

527

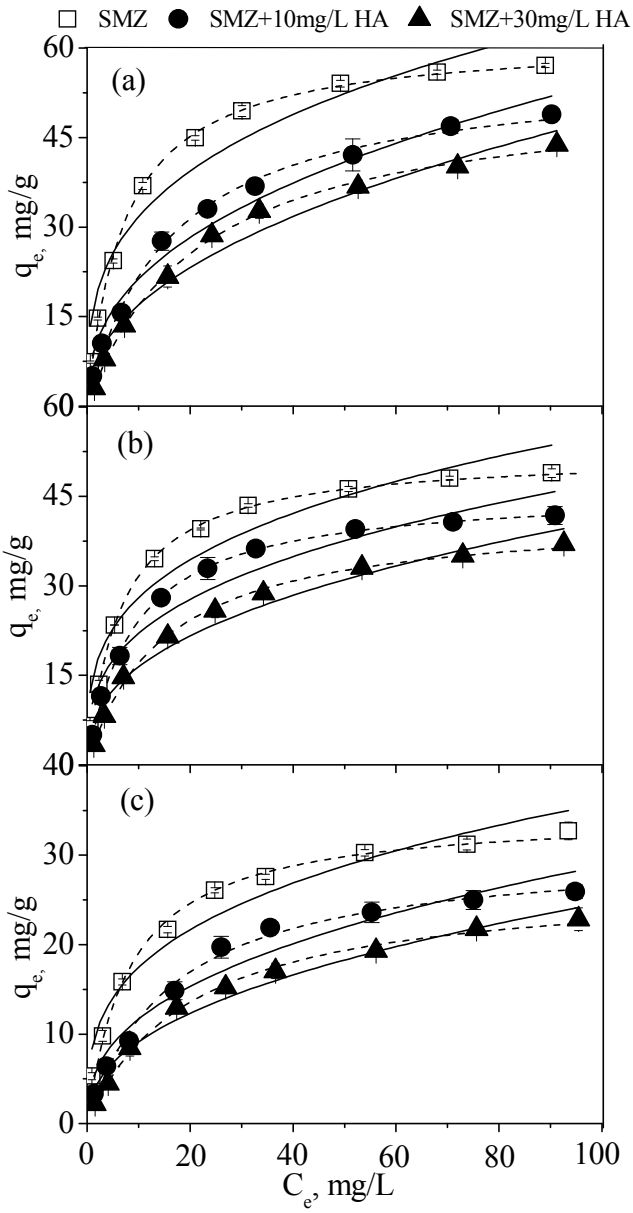

528

529 **Fig. 4.**

530

531

532

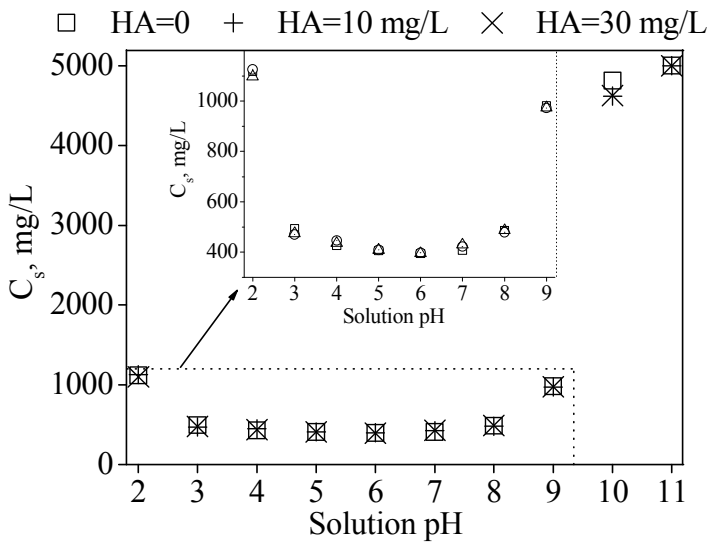

533

534 **Fig. 5.**

535

536

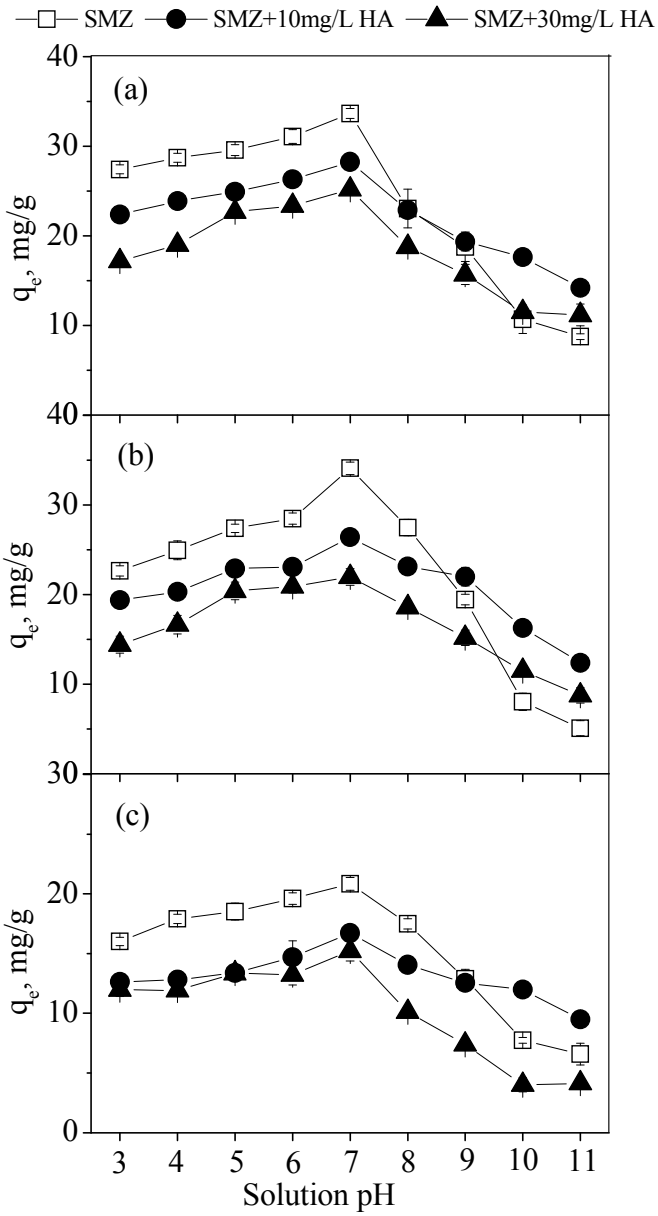

537

538 **Fig. 6.**

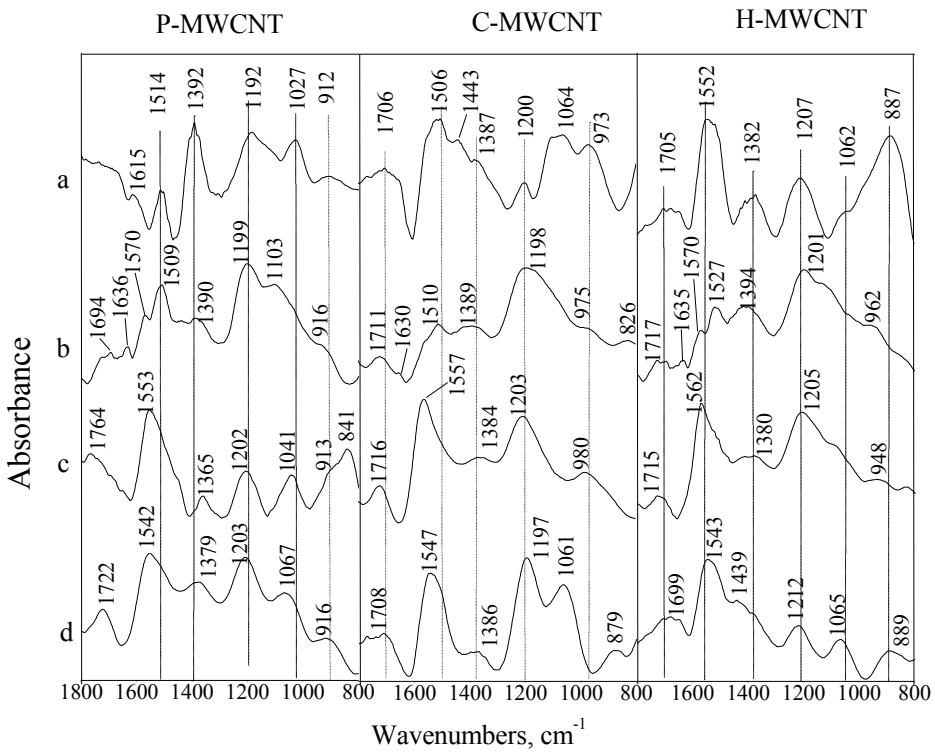

539

540 **Fig. 7.**

Table 1 The Langmuir and Freundlich model fitting adsorption isotherm parameters for adsorption of HA onto three MWCNTs.

Carbons	Langmuir			Freundlich		
	q_{max}[a]	b[a]	R^2	k_F[a]	n^{-1}	R^2
P-MWCNT	171.6±3.6	0.170±0.014	0.995	19.2±4.2	0.430±0.053	0.943
C-MWCNT	152.8±1.4	0.192±0.007	0.998	16.2±3.2	0.457±0.048	0.959
H-MWCNT	135.5±2.6	0.118±0.008	0.996	15.4±2.4	0.444±0.039	0.971

[a]q_{max}: $mg \cdot g^{-1}$; b: $L \cdot mg^{-1}$;k_F:$(mg^{(1-(1/n))} \cdot g^{-1} \cdot L^{(1/n)})$.

Table 2 The Langmuir and Freundlich model fitting adsorption isotherm parameters for adsorption of SMZ onto three MWCNTs.

Carbons	Batch [a]	Langmuir			Freundlich		
		q_{max} [b]	b [b]	R^2	k_F [b]	n^{-1}	R^2
P-MWCNT	A	61.6±0.9	0.138±0.009	0.997	15.50±2.29	0.311±0.039	0.941
	B	56.5±1.6	0.062±0.006	0.994	8.39±1.15	0.405±0.035	0.973
	C	53.1±1.0	0.046±0.002	0.998	5.97±1.01	0.453±0.043	0.968
C-MWCNT	A	52.2±0.7	0.154±0.009	0.997	14.18±2.13	0.295±0.040	0.933
	B	46.0±0.5	0.110±0.004	0.999	10.29±1.69	0.331±0.043	0.937
	C	42.1±0.7	0.068±0.004	0.998	6.63±1.05	0.394±0.040	0.961
H-MWCNT	A	34.7±0.7	0.122±0.010	0.993	8.53±1.11	0.311±0.033	0.953
	B	30.6±1.0	0.062±0.006	0.992	4.74±0.86	0.392±0.033	0.948
	C	27.0±0.6	0.050±0.003	0.997	3.39±0.52	0.431±0.038	0.971

[a] Batch A, B and C indicated without HA, with 10mg·L^{-1} HA and with 30mg·L^{-1} HA,respective;

[b] q_{max}: mg·g^{-1}; b: L·mg^{-1};k_F:($mg^{(1-(1/n))}$·g^{-1}·$L^{(1/n)}$).